Research papers

Impact of dam development and climate change on hydroecological conditions and natural hazard risk in the Mekong River Basin

Jie Yang[a,b], Y.C. Ethan Yang[b], Jianxia Chang[a,*], Jiaorui Zhang[b], Jun Yao[c]

[a] State Key Laboratory of Eco-hydraulics in Northwest Arid Region, Xi'an University of Technology, Xi'an 710048, China
[b] Department of Civil and Environmental Engineering, Lehigh University, Bethlehem, PA, USA
[c] Hanjiang – to – Weihe River Valley Water Diversion Project Construction Co. Ltd., Shaanxi Province, Xi'an 710010, China

ARTICLE INFO

ABSTRACT

The Mekong River Basin, one of the largest river basins in Asia, is facing a great challenge to meet escalating water, food, and energy demands due to rapid development. Meanwhile, climate change and dam development intensify the security issues of these water-related resources. These changes have resulted in flow regime variations that may affect local hydroecological conditions (HEC) further influencing the ecosystem and have resulted in potential economic losses (especially agricultural losses caused by natural hazards). This study explores the impacts of dam development and climate change on baseline local HEC and natural hazard risk (NHR) using a coupled agent-based model that simulates interactions between autonomous agents in the whole basin. A cross-system analysis between the impact on baseline HEC and NHR is conducted to inform future policy in this transboundary basin. The impact on baseline HEC is evaluated from the flow regime variation perspective based on the Range of Variability Approach and the Indicators of Hydrologic Alteration. The impact on NHR depends on variations in the risk of lowest flow and peak flow. The results primarily show that HEC and NHR in the upstream region are more sensitive to precipitation change. The negative impact on baseline HEC by joint dam development and climate change is more significant in the upstream region as well. Under the "hot and dry" climate condition, dam development can potentially mitigate both ecological and economic "loss" in the middle and downstream regions: Central and Southern Laos, the Kratie area, and Mekong Delta, if additional storage can be used in a flexible manner.

1. Introduction

The Mekong River is a transboundary river with an important role in Asia. Water and energy demands in the basin have increased with economic development, industrialization, and a growing population (Dugan et al., 2010; Lacombe et al., 2014; Räsänen et al., 2012). To better meet growing demands for water and energy, many dams have been constructed and planned (Grumbine, 2018; Mekong River Commission, 2010; Pittock et al., 2016). Although there are many debates about dam development, including the impact of upstream dam development on downstream water flow, sediment flow, and ecological concerns (Kuenzer et al., 2013; Räsänen et al., 2012), riparian states still consider hydroelectricity a cheap way to satisfy growing energy demands. Efforts have been made to quantify the impact of dam development in the Mekong River Basin (MRB). On one hand, the positive effects of dam development include energy generation, recreation, and the regulation of streamflow for human water uses. These positive

effects can somewhat compensate for the hazards caused by extreme hydrologic events (Lacombe et al., 2014). On the other hand, flow regulation alters natural flow and changes HEC, which negatively affects some benefits that humans gain from ecosystems (i.e., the ecosystem services provided by ecosystems), such as the fish stock, wildlife habitat, and biodiversity (Dugan et al., 2010; Intralawan et al., 2018; Kummu and Sarkkula, 2008).

The effects of climate change add another layer of concern to regional water and energy security (Economist Intelligence Unit, 2017; Kingston et al., 2011; Trisurat et al., 2018). Several previous studies have assessed the impact of climate change in the MRB. For example, Shrestha et al. (2013) used the soil and water assessment tool (SWAT) to evaluate climate change impacts on sediment in Northern Laos by four general circulation models (GCMs). They found that annual streamflow would change from 17% decrease to 66% increase and resulted in 27% decrease to 160% increase changes in annual sediment yield. Shrestha et al. (2016) evaluated groundwater resource variations
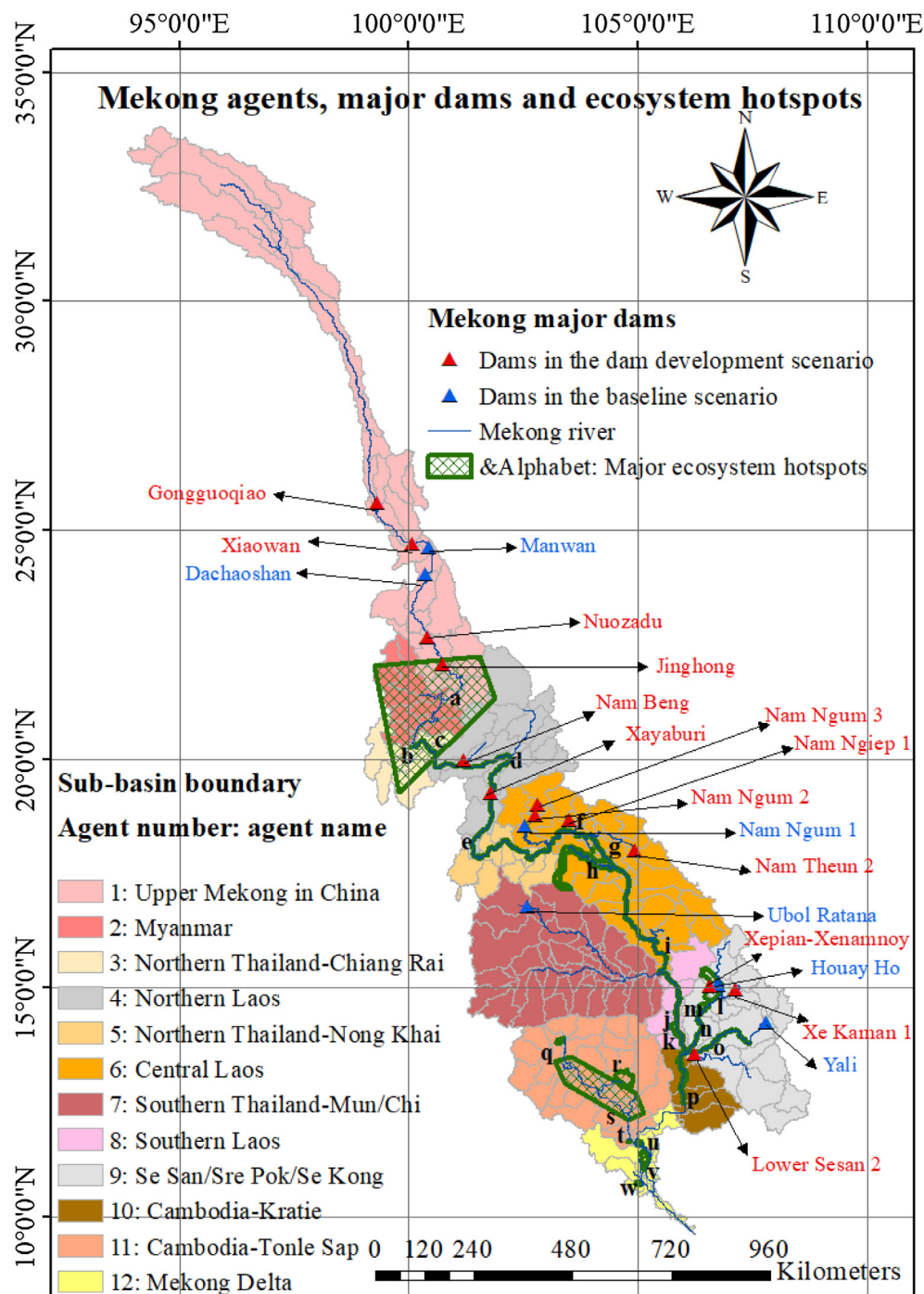
Fig. 1. Locations of agents, major dams, and ecosystem hotspots in the Mekong River Basin. Some ecosystem hotspots (marked with green polygon) are fairly small and are not visible in the basin map. Therefore, all hotspots are further marked with the alphabet.

as a result of climate change and showed declines in future ground-water levels in the Mekong Delta. Vu et al. (2018) simulated seawater intrusion under climate change in the Mekong Delta of Vietnam and estimated that a sea level increase of 30 cm would affect 30,000 ha agricultural area. Kontgis et al. (2019) appraised the impact of climate change on rice productivity and noted that even more water and fertilizers could not offset the yield loss.

Evaluating the joint impact of dams and climate change in large river basins is common around the world such as for the Indus River Basin (Yang et al., 2016), the Carpathian River (Kędra and Wiejaczka, 2018), and the Yuan River (Wen et al., 2018). For the MRB, Le et al. (2007) stated that global warming and dam construction might worsen

flooding in the Mekong River Delta. Ngo et al. (2018) investigated the joint impact on such a hydrological regime in the Lower Mekong Basin and reported that climate change might reduce flow changes caused by dams in the wet season, while it might increase changes in other months. Shrestha et al. (2018) quantified the joint impact on sediment outflow in the Nam Ou River Basin in Northern Laos and concluded enhanced dam sediment management was required. Hoang et al. (2019) depicted the impact on seasonal flow in the whole MRB and concluded that cumulative impacts would intensify the flow decrease in the early wet season.

The MRB is the largest fishery, and is among the most uniquely biodiverse regions in the world (Dugan et al., 2010; Piman et al., 2012).

Agriculture and fishery can be seen as two key ecosystem services that local people depend on for livelihoods and income (Anh et al., 2018; Dugan et al., 2010; Intralawan et al., 2018; Yu et al., 2019). In river ecosystems, hydroecological conditions (HEC) play an important role (Li et al., 2017). HEC reflects multiple streamflow characteristics, such as the magnitude and timing of extreme high/low discharge and the frequency and duration of the high/low pulse, which is critical to sustain the fish life history and production (Yen et al., 2008). Therefore, assessments of major concerns for MRB dam development and climate change should target impacts on HEC and the natural hazard risk (NHR), which directly affects crop production and potential economic losses (Ringler et al., 2011). Also, since MRB is a transboundary river basin, the assessment of HEC and NHR should not follow the "maximizing basin-wide benefit" strategy (Jalilov et al., 2015; Yu et al., 2019). For example, upstream countries enhancing hydroelectricity will influence the downstream HEC, further affecting the ecosystem services (Li et al., 2018). Those countries who lose benefits may consider the outcome to be unfair, which may also worsen geopolitical conditions (Yu et al., 2019). Therefore, these impact analyses should consider both different regions and the whole basin (Keskinen et al., 2015; Pittock et al., 2016; Yang et al., 2016).

Based on the outline above, the primary goal of this study is to simultaneously assess dam development and climate change impacts on HEC and NHR as compared to the baseline; then we conduct a cross-system analysis between the impact on baseline HEC and NHR for comprehensive tradeoff analyses among different regions (dividing MRB into different stakeholders). This study can be seen as an initial effort at concurrent regional and cross-system tradeoff analysis in the MRB. Different stakeholders in the MRB may have different interests and water use preferences, because different departments compete with each other for limited water resources. To conduct the tradeoff analysis, an agent-based model (ABM; used for dividing the MRB into different self-organized regions to better reflect real-world human interventions in each region) coupled SWAT model (utilized for simulating streamflow) previously developed by Khan et al. (2017a) is employed for the complex human and natural water system. The outcome of this study can be used to inform policies in different regions based on dam impacts on baseline local aquatic ecosystems and potential economic losses.

2. Study area, data, and scenarios

2.1. MRB in the coupled ABM-SWAT model

The Mekong River originates in Tibet and flows through China, Laos, Myanmar, Thailand, Cambodia, and Vietnam before entering the South East Asia Sea (Fig. 1). It is one of the largest rivers in Asia, with a length of approximately 4800 km and a drainage area of 795,000 km². Rapid dam development and the changing environment may lead to HEC changes and local ecosystem service losses as a result of changing flow regimes. Twenty-three ecosystem hotspots (mostly wetlands) are identified by local ecological experts in WorldFish based on species richness, number of species at risk, existing protection schemes, and area sensitivity (Baran et al. 2015, Fig. 1 and Table S1 in supplementary materials). HEC changes in these hotspots will notably affect aquatic habitats, fish biodiversity, and spawning grounds; so they are selected as analysis targets in this study. We also divide the entire MRB into 12 regions based on political boundaries and natural catchment boundaries. First, we divide the basin by political boundaries. Among each country, the basin is further divided by the natural catchment boundaries. These 12 regions are defined as "water use agents" in the ABM, following the settings in Khan et al. (2017a) to evaluate the impact on NHR.

2.2. Data and scenarios

This study identifies a series of potential uncertain scenarios to explore the impact of different dam development and climate change conditions. In the MRB, numerous dams are under construction (Räsänen et al., 2018). In this study, we select a total of 19 major dams (dams already being operated, and those dams will be completed around 2020) based on volume (with relatively large storage) and, most critically, data availability in the MRB to assess the dam development impact. All 19 dams (6 in China, 10 in Laos, 1 in Thailand, 1 in Vietnam, and 1 in Cambodia) generate hydroelectricity, while only one dam (Ubol Ratana located in Thailand) is also used for irrigation. The characteristics (country ownership, status, storage, and purpose) of the 19 modeled dams are shown in Table S2 (in supplementary materials). As our available data period is from 1983 to 2007, we consider 6 dams (all completed and operated before 2007) as the baseline dam scenario (with total storage of 12,463 million cubic meters, MCM). And, in total 19 dams are modeled with the total storage of 76,215 MCM in the dam development scenario (Fig. 1).

Climatic drivers that may affect the streamflow include precipitation, temperature, wind, humidity, vapor pressure, solar radiation, and others (Tian et al., 2018). Precipitation (P) and temperature (T) are the two main climatic drivers considered in this study. Several previous studies have quantified the impact of climate change on future precipitation and temperature across the MRB (Hasson et al., 2016; Hoang et al., 2016; Shrestha et al., 2016). In general, precipitation and temperature projections vary with representative concentration pathways (RCPs) and GCMs. Based on future precipitation and temperature projections of these available studies, we conduct a climate stress test with five precipitation change levels (P $+0\%$, $+15\%$, $+30\%$, -15%, and -30%) and four temperature change levels (T $+0\,°C$; $+1.5\,°C$; $+3\,°C$; and $+4.5\,°C$) to cover the possible range of future climate conditions (Brown et al., 2012). The tested temperature increase scenarios fit with the RCP 2.6 ($1.5\,°C$) and RCP 8.5 ($3\,°C$) projections for the period of 2050–2093 under the ensemble GCM results tested by Ruan et al. (2019). Changes in precipitation and temperature are applied to daily historical data (period from 1983 to 2007). Precipitation data is obtained from the Asian Precipitation-Highly Resolved Observational Data Integration Towards the Evaluation of Water Resources project (Yatagai et al., 2012), and temperature data is obtained from the National Centers for Environmental Prediction Climate Forecast System Reanalysis (NCEP-CFSR, Saha et al., 2010). Therefore, 40 scenarios are considered in this study as a joint dam and climate sensitivity test, which consist of 2 dam development scenarios and 20 (4×5) climate change conditions (Table S3 shown in supplementary materials). The scenario containing the baseline dams (6 dams) with no precipitation or temperature changes is defined as the baseline scenario.

Other data required to run the coupled ABM-SWAT model include reservoir characteristics (such as operational rule, and storage), geographic linkages of different agents and ecosystem hotspots, elevation obtained from the SHuttle Elevation Derivatives at multiple Scales (HydroSHEDS) database, land use obtained from Spatial Production Allocation Model (SPAM) database for 2005, land cover obtained from the Global Land Cover 2000 database, soil (from the FAO/UNESCO), cropped area (estimated based on the SPAM database), and meteorological data such as solar radiation, wind speed, humidity obtained from NCEP-CFSR with the data period from 1983 to 2007.

3. Methods

3.1. Coupled ABM-SWAT model

The coupled ABM-SWAT model developed by Khan et al. (2017a) is used for cross-system analysis between HEC and NHR. The ABM allows each agent to make its own behavior rule about the water use preferences (agricultural irrigation, hydroelectricity generation, or water for ecosystem health) in the MRB. By considering the behavioral rule in each agent, this coupled modeling framework reflects real-world human adaptive decisions better than a simple process-based

hydrological model. The water use preferences of each agent are determined and set based on a comprehensive E-survey (Khan et al., 2017b). Water use rankings in each agent are shown in Table S4 in supplementary materials.

In the SWAT model, the 12 agents in the basin are further divided into 289 sub-basins to better simulate the spatial variations of hydrologic process (Fig. 1). Each sub-basin has several hydrological response units with similar soils, land use/land cover, and slope, which are then used to simulate runoff generation. The SWAT is calibrated (period from 1983 to 1992) and validated (period from 1993 to 2007) based on streamflow data obtained from L'Institut de recherche pour le développement. The Nash-Sutcliffe coefficient of the SWAT calibration and validation for ten gauging stations are mostly over 0.8, indicating a relatively good performance of the model (Khan et al., 2017a).

Besides running the SWAT model following the behavioral rules set in ABM, this coupled model also allows each agent to observe the impact of their behavior rule and to make corresponding changes based on the output in SWAT. The two-way coupled model can better represent the interaction between the nature and human. The ABM and SWAT models interact on an annual time scale. At the end of each year, agents update their decisions on dam operations and crop area based on the comparisons between SWAT outputs (such as streamflow, crop yield, reservoir storage, and release) from that year and the initial target setting. For example, if agriculture production ranks first and the actual crop production is lower than the target, the agent will increase the irrigated area. If hydropower generation ranks first, and the actual production is smaller than the target, agent will decrease number of days to reach the target dam storage. However, if the ecosystem health ranks first and the streamflow does not reach the target, the agent will not take any measures no matter crop and hydropower production reach their targets or not. Then, the SWAT model uses the new settings to simulate the runoff for the coming year. The model workflow and more technical details for the coupled model can be found in Khan et al. (2017a).

3.2. Calculation of impact on baseline HEC

This study uses the flow regime variation to reflect the impact on baseline HEC. First, the Indicators of Hydrologic Alteration (IHA) method, including 33 hydroecological parameters (Richter et al., 1996, 1998), is selected. These parameters represent different aspect of flow conditions that can potentially influence the ecosystem. For example, the 7-day annual maximal and minimal flow are well-known descriptors of dam impact as well as the 30-day annual maximal and minimal flow reflect dry or wet years in the MRB (Baran et al., 2015). More general interlinks between IHA parameters and corresponding ecosystem influences can be found in Table S5 in supplementary materials. Then, the Range of Variability Approach (RVA; Richter et al., 1997) is employed to assess the flow regime change by analyzing variations of the 33 IHA parameters under different climate and dam development scenarios compared to the baseline.

We acknowledge that IHA/RVA are intended to start with a natural flow regime as the baseline to represent potential deviation from desired ecological state. However, given the data availability is after 1983 in this study, the truly "natural flow regime" for the MRB is difficult to assess. To inform policy, we alternatively define the flow condition from 1983 to 2007 as a "baseline" scenario and then compare the flow condition under climate change and/or dam development condition with the baseline. In this setting, we assume higher flow regime variation that is, HEC away from the baseline is less desirable and may lead to more serious "potential" ecosystem degradation and ecological "loss."

We use the following four steps to compute the impact on baseline HEC for each ecosystem hotspot in the MRB.

(1) Determine the baseline flow condition. In this study, the output of

the ABM-SWAT model under the baseline scenario is defined as the baseline flow condition. Then, 33 IHA parameters values for each year at each hotspot are calculated based on the baseline daily streamflow data inside the boundary of the hotspot.

(2) Determine the environmental flow target of each IHA parameter. Following Richter et al. (1997), the 25th and 75th percentile ranges of multiyear IHA parameter values under the baseline scenario (calculated in step 1) are selected as the flow target to maintain the baseline local HEC.

(3) Run the ABM-SWAT model for altered climate and dam development scenarios and calculate the 33 IHA parameters for each year at each hotspot in these 39 scenarios.

(4) Calculate the hydrologic alteration degree to quantify the flow regime variation (Richter et al., 1998). The hydrologic alteration degree (HAD_i) of each IHA parameter is evaluated as follows:

$$HAD_i = \left(\frac{Nas_i - Nbs_i}{Nbs_i} \right) \times 100\% \tag{1}$$

where HAD_i is the hydrologic alteration degree of ith IHA parameter in the future scenario compared to the baseline scenario; Nas_i is the number of years for which the multiyear IHA parameter values under the altered climate change and dam development scenarios (obtained in Step 3) falling into the baseline environmental flow target; and Nbs_i is the number of years for which the multiyear IHA parameter values under the baseline scenario (obtained in Step 1) falling into the baseline environmental flow target.

The hydrologic alteration degree varies with the IHA parameter (Shiau and Wu, 2004). Some values may increase while others may decrease. It is difficult to directly use 33 IHA parameters at the same time to assess the tradeoffs between HEC and NHR for policy makings. Therefore, in this study, we use Eq. (2) to calculate the comprehensive hydrologic alteration degree (*CHAD*, which is the mathematical definition of impact on baseline HEC compared to the baseline scenario in this study) considering 33 IHA parameters in future scenarios compared to the baseline scenario:

$$CHAD = \sqrt{\frac{\sum_{i=1}^{33} HAD_i^2}{33}} \tag{2}$$

This mathematical mean summarizes ecologically relevant flow alterations, giving us a common standard for comparison across hotspots. However, it does not, in itself, give any indication of the actual ecological state of a system; actual potential ecosystem states that may arise from specific IHA parameter values need further investigation with more detailed ecological studies. Following Richter et al. (1998), the *CHAD* value ranges from 0 to 100%, while larger *CHAD* value indicates that HEC is away from the baseline and less desired. A value of 0% means no change from baseline (again, not natural flow regime but baseline), and 100% means complete change from baseline.

3.3. Calculation of impact on NHR

In this study, we focus on two natural hazards: the lowest flow in the dry season and the peak flow in the wet season, both having major impacts on agricultural productivity and economic development (Economist Intelligence Unit, 2017). We use the change in NHR to reflect the potential impact of both lowest flow and peak flow events on economic losses. NHR is statistically defined as the occurrence probability of the streamflow higher (or lower) than a threshold in this study. To compare the impact on NHR at each agent, the risk (both lowest flow and peak flow) of the baseline scenario for each agent is assigned to be the same. This concept is similar to the identification of hydrologic events by the streamflow drought index (SDI), a widely applied hydrological drought index calculated based on long-term streamflow data including both wet and dry period (Nalbantis and Tsakiris, 2009). This index is analogous to the standardized
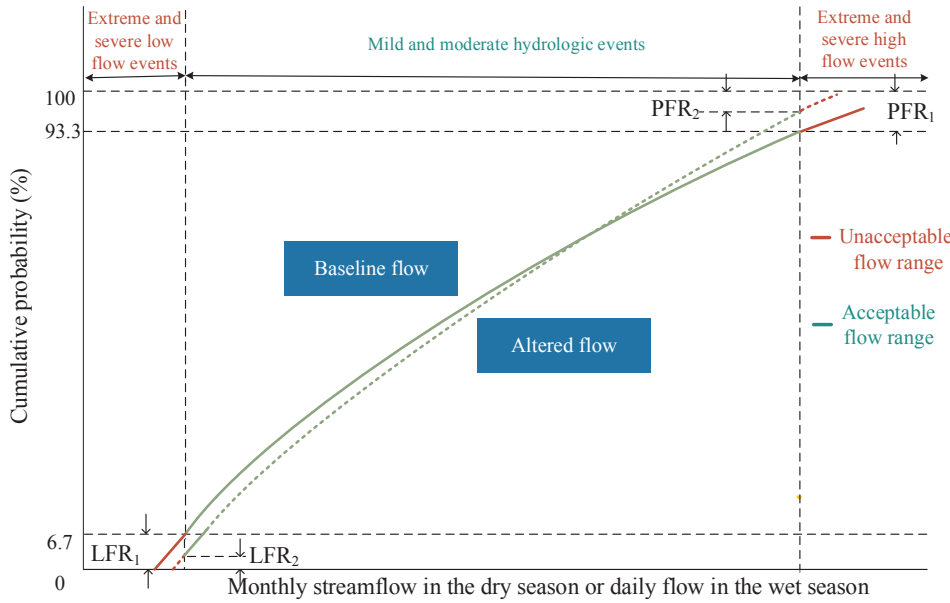
Fig. 2. Calculation of natural hazard risk variation. X-axis reflects streamflow value (monthly streamflow in the dry season or daily streamflow in the wet season). Y-axis is natural hazard cumulative probability (%). Solid and dash lines represent the baseline flow and altered flow, respectively. Abbreviations: LFR$_1$ and PFR$_1$: risk of unacceptable lowest flow and peak flow events for baseline flow (equal to 6.7%), respectively. LFR$_2$ and PFR$_2$: risk of lowest flow and peak flow events for altered flow, respectively.

precipitation index (SPI; a normalized index), and the low flow event and high flow event can be represented similarly (Angelidis et al., 2012). Following the SDI concept, hydrologic events can be characterized as: "extreme," "severe," "moderate," and "mild" (Nalbantis and Tsakiris, 2009). Extreme and severe low flow and high flow events (hydrologic events that may lead to higher economic loss compared to other kinds of events) both have an occurrence probability of 6.7%. This also indicates that extreme and severe low flow events have a flow value with a cumulative probability smaller than 6.7%, while the extreme and severe high flow events have a flow value with a cumulative probability higher than 93.3% (Fig. 2).

In this study, we separate the dry and wet season to identify the lowest flow and peak flow as flow patterns in the Mekong are entirely different for wet and dry seasons (Intralawan et al., 2018). For easy calculation, we assume the dry season is from January to June, and the wet season is from July to December for all 12 agents. The streamflow for each agent is divided into two ranges: acceptable and unacceptable (Fig. 2). Unacceptable events are the lowest flow and peak flow with the occurrence probability equal to 6.7% based on the SDI concept. This also indicates that the occurrence probabilities (i.e., risk defined in this study) of lowest flow and peak flow are both 6.7% in the baseline scenario.

A four-step process is used to calculate the impact on NHR for each agent.

1) Determine the best-fit probability distribution function of the baseline flow. In general, peak flow affects ecosystem and human society by a fast and relatively short-term process, while the lowest flow will have a slow and long-term effect (Van Loon, 2015). Due to these different characteristics, we use the daily flow data for peak flow risk (PFR) calculation and monthly flow data for the lowest flow risk (LFR) calculation (data series both from 1983 to 2007). First, four probability distribution functions, including Gamma, Weibull, Rayleigh, and Lognormal, are employed in this study as candidates to fit the flow distribution (daily flow in the wet season or monthly flow in the dry season). The best-fit function is determined based on the root mean square error (RMSE), which reflects the difference between the theoretical cumulative probability (P_t) and empirical cumulative probability (P_e), shown in Eq. (3):

$$RMSE = \sqrt{\frac{1}{n-1} \sum_{i=1}^{n} (P_e - P_t)^2}$$

(3)

Lower *RMSE* value is better, because P_t has a better ability to match P_e. P_e is calculated by the Gringorten formula in Eq. (4) (Gringorten, 1963):

$$P_e = P(X \le x_i) = \frac{\sum_{m=1}^{i} N_m - 0.44}{n + 0.12}$$

(4)

where N_m is the number counted as $X \le x_i$; x_i is the streamflow value; and n represents the total number of streamflow data. The values 0.44 and 0.12 in Eq. (4) are empirical constraints (Gringorten, 1963).

The equations to calculate the P_t of Gamma, Weibull, Rayleigh, and Lognormal are shown in Eqs. (5)–(8), respectively:

$$P_t = F(x|\ a, b) = \frac{1}{b^a \Gamma(a)} \int_0^x t^{a-1} e^{\frac{-t}{b}} dt$$

(5)

$$P_t = F(x|\ b, a) = \int_0^x ab^{-a} t^{a-1} e^{-(\frac{t}{b})^a} dt$$

(6)

$$P_t = F(x|\ b) = \int_0^x \frac{t}{b^2} e^{(\frac{-t^2}{2b^2})} dt$$

(7)

$$P_t = F(x|\ u, \sigma) = \frac{1}{\sigma\sqrt{2\pi}} \int_0^x \frac{e^{\frac{-(\ln(t)-u)^2}{2\sigma^2}}}{t} dt$$

(8)

where x is the streamflow value; a is the shape parameter; b is the scale parameter; and u and σ are the mean and deviation of the streamflow values, respectively. The parameters of each distribution function are estimated by a MATLAB function.

2) Determine the acceptable and unacceptable flow range (diagram shown in Fig. 2). Based on the determined best function for the baseline flow in Step 1, the upper streamflow value of the unacceptable lowest flow event, that is, lower acceptable flow value (LAF), is calculated by the cumulative probability of 6.7%, and the lower streamflow value of the unacceptable peak flow event, that is, the upper acceptable flow value (UAF), can also be computed by the cumulative probability of 93.3%.

3) Run the ABM-SWAT model for altered climate and dam development scenarios and determine the best-fit distribution function (similarly as in Step 1) and the corresponding parameters of the rest of the 39 scenarios.

4) Based on the upper/lower streamflow value of the unacceptable lowest flow/peak flow event (determined in Step 2) and the best-fit distribution function of the altered flow (determined in Step 3),
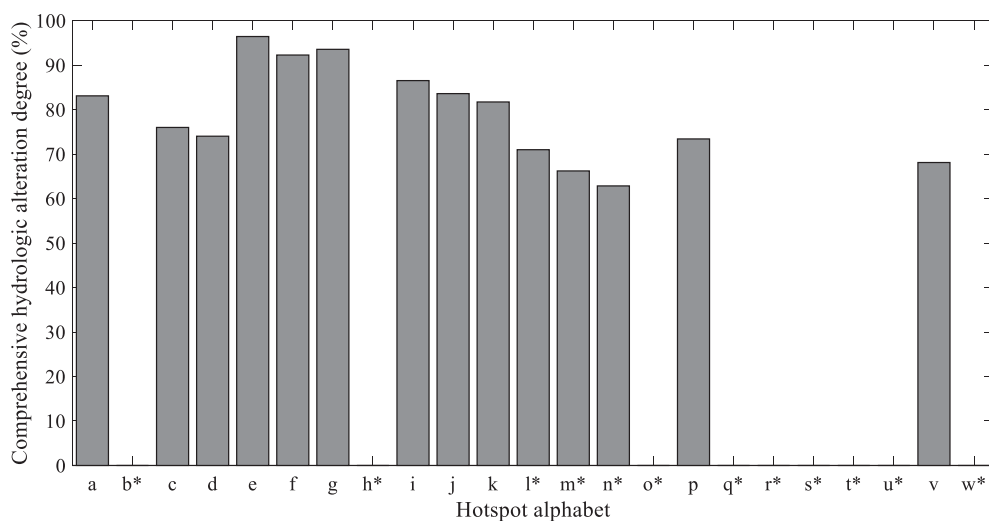
Fig. 3. Dam development impact on the *CHAD*. X-axis indicates hotspot alphabet basically from upstream to downstream, while * indicates hotspot at the tributary. Y-axis is the *CHAD*. Larger *CHAD* value is less desired because HEC is away from the baseline. Hotspots with a value of 0 indicates no impact of further dam development.
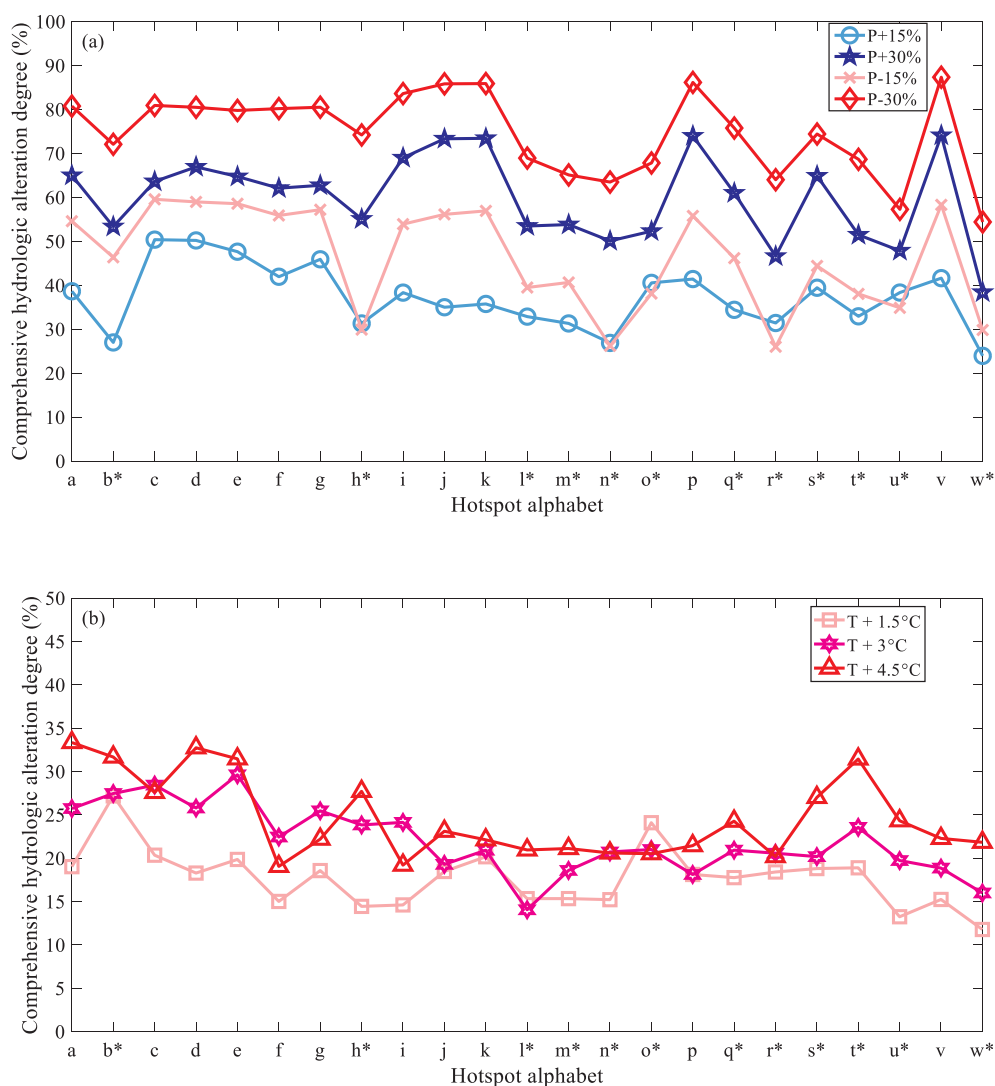

Fig. 4. Climate change impact on the *CHAD*: (a) impact of precipitation and (b) impact of temperature. * indicates hotspot at the tributary. In Fig. 4(a), blue colors (from light to dark) represent precipitation increase levels, and red colors (from light to dark) represent precipitation decrease levels. In Fig. 4(b), red colors (from light to dark) represent temperature increase levels. Abbreviations: P, precipitation; T, temperature. (For interpretation of the references to colour in this figure legend, the reader is referred to the web version of this article.)

calculate the upper/lower cumulative occurrence probability of the unacceptable lowest flow/peak flow event for the altered climate change and dam development scenarios (Fig. 2). Then, calculate the occurrence probabilities (the mathematical definition of NHR in this study) of the unacceptable lowest flow and peak flow events under the altered climate change and dam development scenarios (LFR2 and PFR2 shown in Fig. 2). The LFR and PFR calculation equations are shown in (9) and (10), respectively.

$$LFR = upper\ cumulative\ probability\ of\ lowest\ flow \quad (9)$$

$$PFR = 100 - lower\ cumulative\ probability\ of\ peak\ flow \quad (10)$$

4. Results

4.1. Impact on baseline HEC

4.1.1. Dam development impact on baseline HEC

Fig. 3 demonstrates *CHAD* values that quantify the change of HEC under dam development without climate change condition. The *CHAD* value is plotted on the y-axis, and ecosystem hotspots are on the x-axis. Note that ecosystem hotspots are ordered alphabetically from left to right, which is approximately upstream to downstream, not in chronological order. Larger *CHAD* value means HEC is away from the baseline and is less desirable.

The impacts on mainstream hotspots HEC are somewhat higher than those in the tributaries. This is because more dams with higher storage are located upstream of mainstream. Higher dam regulation capacity leads to higher streamflow variation and flow regime change. Among the hotspots in the tributaries, HEC in Hotspot "l"," "m," and "n" is affected because there are two dams (Xepian-Xenamnoy and Xe Kaman 1 with total storage of 7,204 MCM) upstream of these hotspots further considered in the dam development scenario. The *CHAD* values for other hotspots are equal to 0 because there are no dams upstream of these hotspots further considered in the dam development scenario compared to the baseline.

Focusing on the mainstream hotspots, the impact on upstream HEC (Hotspot "a" to "i") is higher than impacts on downstream hotspots (Hotspot "j" to "w"). A possible reason is that more dams are further considered in the dam development scenario compared to the baseline, thus affecting the mainstream flow that upstream hotspots highly depends upon. A majority of streamflow in downstream hotspots coming from tributaries (Li et al., 2017) can mitigate the upstream dam development impact to a certain extent.

4.1.2. Climate change impact on baseline HEC

Fig. 4(a) and (b) demonstrates *CHAD* results under climate change scenarios reflecting the impact of precipitation and temperature change on HEC compared to the baseline scenario. For easy comparison, the scale is the same as that of the baseline scenario in Fig. 3. Following a single line from left to right in Fig. 4(a) correlates to moving downstream, which demonstrates a decreasing trend. Streamflow at tributary hotspots is smaller, but with higher inter-annual variations, compared to those of the mainstream hotspots. This flow pattern results in a relatively larger flow range in the baseline condition to sustain the local aquatic ecosystem health. Therefore, the impact on baseline HEC by precipitation change of these hotspots is lower than that in the mainstream hotspots.

Next, we compare different lines in Fig. 4(a). The results show that impacts on baseline HEC by larger precipitation variation (precipitation ± 30%) are higher than those with lower precipitation variation (precipitation ± 15%), which is expected. Larger precipitation variation leads to larger streamflow changes. In Fig. 4(a), at the same precipitation change condition, precipitation decreases basically result in higher *CHAD* values, which correlates to negative impacts on baseline local aquatic ecosystems. This is because the modeling results show that

river streamflow variations (after being consumed by agricultural irrigation and hydroelectricity generation) are higher in precipitation decrease scenarios than in precipitation increase scenarios. Furthermore, the distances between four *CHAD* lines under four precipitation change conditions are larger in the upstream than those in the downstream. This result indicates that upstream HEC is more sensitive to precipitation change than the downstream. Since the upstream region of the MRB is characterized by narrow and steep gorges (Thompson et al., 2013), terrain causes rapid rise and recession during the hydrological process, limiting the precipitation redistribution capacity. Therefore, with the same precipitation variation percentage, larger flow variation is observed upstream.

Fig. 4(b) demonstrates the impacts of temperature change on baseline HEC from upstream (left) to downstream (right). A declining trend is observed from left to right. Similar to Fig. 4(a), this effect is caused by lower inter-annual variation in streamflow at mainstream hotspots, which then leads to higher *CHAD* values by temperature change. Comparing different temperature change levels in Fig. 4(b), the impact of temperature change on baseline local HEC is not consistent, unlike the pattern of precipitation change in Fig. 4(a). Temperature is an important factor that affects irrigation water demand and crop production in the SWAT model. Different crops have different suitable temperature ranges, and temperature increases lead to inconsistent crop growth and irrigation water demand change, resulting in an inconsistent trend of impact on baseline local HEC by temperature change. In summary, the impact of a temperature increase of +4.5 °C is the highest among the three temperature increase conditions, due to the higher evaporation and higher flow decrease.

4.1.3. Joint impact of dam development and climate change on baseline HEC

The *CHAD* results under two dam development levels, together with 20 climate change levels, are shown in Fig. 5 with the same x- and y-axes as in Figs. 3 and 4. The 20 diagrams refers to 20 climate change levels. In each diagram, the solid line and the dot represent baseline and dam development scenarios, respectively. This figure aims to show the impact on baseline local HEC by precipitation change (column to column comparison), by temperature change (row to row comparison), and by dam development in each climate change diagram (difference of *CHAD* values between baseline and dam development conditions) simultaneously.

Fig. 5 shows that the difference between *CHAD* values under baseline and dam development conditions with no precipitation change (third column) is the highest; this difference gradually decreases with extreme precipitation (first and fifth columns). As shown in Fig. 4(a), precipitation change impact on baseline local HEC without dam development varies significantly, and the impact dramatically increases under P ± 30%. However, Fig. 5 shows that the impact of dam development is greater than that of climate change, resulting in similar *CHAD* values across all precipitation and temperature change conditions, that is, all *CHAD* values under the dam development condition (all dots) are at approximately the same horizontal level. Fig. 5 also demonstrates that the impact of temperature is less distinguishable than precipitation when comparing different temperature scenarios in different rows.

Also, *CHAD* values under dam development conditions are above the values in the baseline dam condition under the P ± 15%, P + 30%, and P + 0% precipitation conditions. This indicates that under these four precipitation change conditions, dam construction may be not a good choice for maintaining the baseline local HEC. However, under the P –30% condition, the difference is smaller than the other four precipitation conditions. Also, *CHAD* values under dam development condition are below those values under the baseline dam condition in Hotspots "I," "j," "k," "m," "n," "p," and "v." These findings indicate that dam construction with larger streamflow regulation capacity may increase the low flow and reduce the streamflow variation degree,
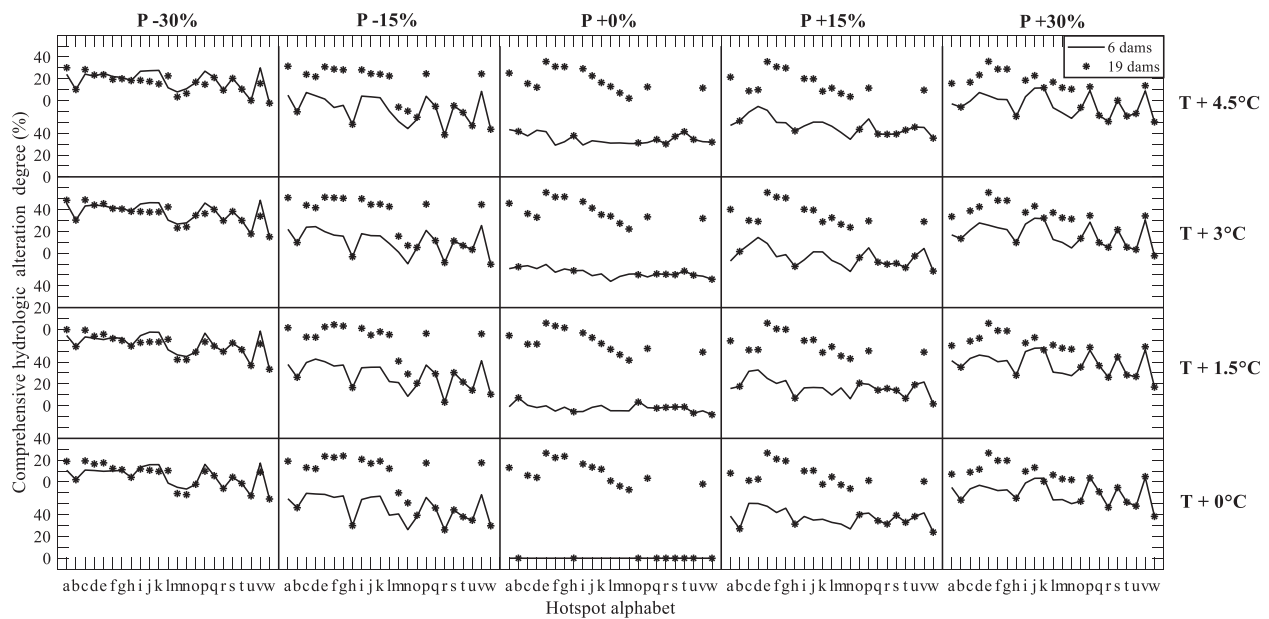
Fig. 5. Joint impact of dam development and climate change on the *CHAD*. Diagrams correspond to 20 climate change conditions. In each diagram, solid line represents results without dam development, and dots represent results with dam development.

which can slightly mitigate the impact of precipitation and temperature change on baseline HEC under extreme precipitation decrease condition in these hotspots.

4.2. Impact on NHR

4.2.1. Dam development impact on NHR

According to the method in Section 3.3, for lowest flow event identification, the best-fit probability distribution function of stream-flow for Agents 7 and 11 in the baseline scenario is Gamma, while that for other agents is Lognormal. For peak flow event identification, the best-fit probability distribution function of streamflow for Agent 9 in the baseline scenario is Gamma, while that for the other agents is Weibull. We use these functions to further calculate the NHR in 39 future scenarios. Fig. 6(a) demonstrates the LAF and UAF for each agent while Fig. 6(b) shows the upper/lower cumulative probability of lowest flow and peak flow for altered flow (LFCP and PFCP, respectively) under the scenario with dam development and no climate change. Higher LFCP represents higher unacceptable LFR while higher PFCP represents lower unacceptable PFR.

Agents 7 and 11 are located at the tributaries; the NHR in these two agents is not affected by dam development (LFCP and PFCP equal to 6.7% and 93.3%, respectively; same with the values in the baseline scenario). For the other ten agents, LFCP values are all smaller than 6.7% and PFCP values are all higher than 93.3%, meaning LFR and PFR decrease with dam development due to the higher streamflow regulation capacity of more dams. These findings are consistent with some previous studies (Lacombe et al., 2014; Lauri et al., 2012; Matthews and Motta, 2015; Piman et al., 2012).

The LFCP values in each agent affected by dam development are approximately 0 for all, while the PFCP values are all over 96.6%. When we compare PFCP with 93.3%, the PFR decrease in the upstream agents is relatively less. This is because most dam developments are placed upstream with higher storage increase. More dams mainly used for hydroelectricity generation may lead to relatively lower water release variation and lower PFR variation, which highly depends on main-stream flow.

4.2.2. Impacts of climate change on NHR

Fig. 7(a) and (b) demonstrate the impact on LFR and PFR under

future precipitation change scenarios, without temperature change or dam development. The x-axis shows the agent number (approximately upstream to downstream from left to right but not the chronological order), while the y-axis represents the NHR value (the occurrence probability of unacceptable events). Larger NHR values may lead to larger potential economic losses. Precipitation decrease results in increased LFR (Fig. 7a) and decreased PFR (Fig. 7b) as expected and vice versa.

Next, we focus on NHR variation between a single bar (either precipitation decrease or increase) with the precipitation remained unchanged bar. From left to right, the same precipitation change results in higher LFR (red bars) and PFR (blue bars) variations in the upstream agents when compared to the downstream agents. These results suggest that NHR variation in the upstream is more sensitive to precipitation, possibly due to the upstream steep terrain characteristic, resulting in larger hydrologic variations.

4.2.3. Impacts of climate change and dam development on NHR

The LFR and PFR results under two dam development scenarios, together with 20 climate change levels (i.e., 40 scenarios), are shown in Fig. 8 with the same x- and y-axes as Fig. 7. In each diagram, solid red and blue lines represent the results of LFR and PFR, respectively, when no additional dam is considered. Dash red and blue lines represent the results of LFR and PFR, respectively, with future dam development. Again, the x-axis represents agent order, basically from upstream to downstream rather than in the chronological order.

Under the precipitation decrease conditions, LFR decreases with dam development, and the difference between lowest flow risk under baseline and dam development condition under the P −30% condition is the largest, and it gradually approaches the no precipitation change scenario (third column). Therefore, the reduction of LFR by dam development under P −30% is the highest, because the larger capacity of dams further increases low flow when precipitation decreases. Similarly, under the precipitation increase conditions, PFR decreases with dam development. In addition, the difference of PFR between the baseline and dam development condition for P +30% condition is the largest, and it gradually approaches the P +0% scenario. Higher regulation capacity of dam development is mostly beneficial when streamflow increases, as more dams can further decrease the high flow. In Fig. 8, the difference between the natural hazard risk (no matter
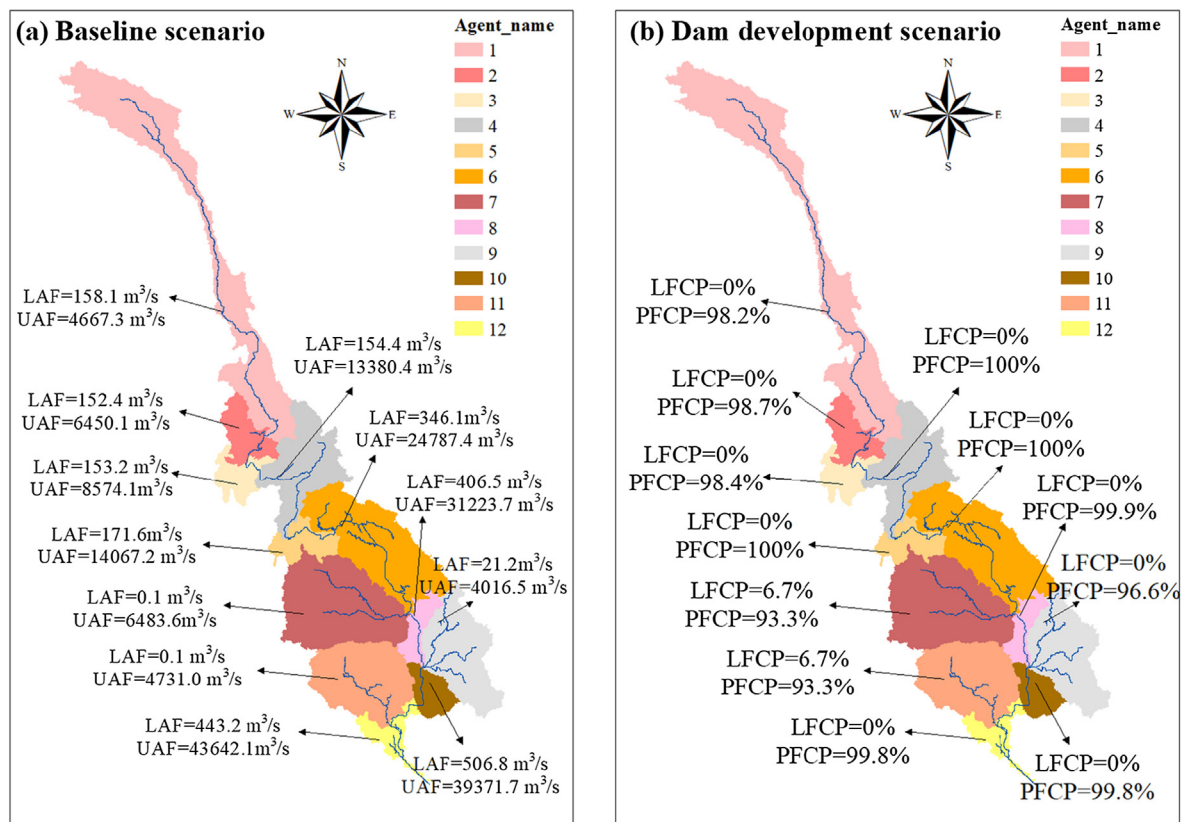
Fig. 6. Dam development impact on natural hazard cumulative probability. Abbreviations: LAF and UAF: lower and upper acceptable flow values, respectively. LFCP and PFCP: cumulative probability of lowest flow and peak flow for altered flow, respectively.

under baseline or dam development condition) in different rows is hardly visible, indicating that the temperature impact on NHR variation is very small.

5. Discussion

5.1. Cross-system analysis between HEC and NHR to inform policy

To quantify the tradeoffs between HEC and NHR under dam development and climate change, we label each hotspot (where the most downstream sub-basins located) into an agent and calculate the average *CHAD* for each agent. Because there are no hotspots in Agents 2, 5, and 7, and dam development will not affect Agent 11, this tradeoff analysis only focuses on Agent 1 (Upper Mekong in China), Agent 3 (Northern Thailand-Chiang Rai), Agent 4 (Northern Laos), Agent 6 (Central Laos), Agent 8 (Southern Laos), Agent 9 (Se San/Sre Pok/Se Kong), Agent 10 (Cambodia-Kratie), and Agent 12 (Mekong Delta).

Fig. 9 demonstrates the tradeoff analysis among *CHAD*, LFR, and PFR for those selected agents under two extreme climate change conditions. The left subplot demonstrates the temperature increase (+4.5 °C) and precipitation increase (+30%) for the "hot and wet" condition. In this condition, we focus on peak flow events. The right subplot demonstrates the temperature increase (+4.5 °C) and precipitation decrease (−30%) for the "hot and dry" condition and we focus on lowest flow events. Since it is unlikely that the temperature will go down, we only test these two extreme climate conditions. Different colors represent different agents. The symbols "o" and "x" indicate results under baseline and dam development scenarios, respectively. Therefore, moving from symbol "o" to "x" reflects the impact of dam development. Since the highest values of all these axes are negative, movement toward to the left bottom is ideal (the star).

In the left subplot (Fig. 9a), all agents have movements toward the upper-left, this indicates that dam development reduces PFR but causes

CHAD increase in all regions. These results indicate that all regions have to trade the economic "benefit" (reduced PFR) with ecological "cost" (increased *CHAD*).

In Fig. 9b, similar horizontal movements to the left are observed. Therefore, dam development can mitigate LFR under the "hot and dry" scenario for all agents. However, unlike Fig. 9a, *CHAD* values in different agents show different movements in the "hot and dry" condition. The *CHAD* values in Agents 1, 3, and 9 show upward movement (in the magnitude of 6%) indicating these agents do need to further consider the tradeoffs between ecological "cost" (increased *CHAD*) and economic "benefit" (reduced LFR) especially Agent 1. The *CHAD* values in Agent 4 basically remain unchanged and in Agent 6, 8, 10, and 12 show downward movement meaning these agents do not have the tradeoff between ecological "cost" and economic "benefit" by dam development under this future climatic condition.

It is noteworthy that the storage increase in dam development scenario in Agent 1 (Upper Mekong in China) is the highest, it will also suffer more ecological "loss" among these 8 agents in the tradeoff analysis under these two extreme climate change conditions. In addition, dam development impact on baseline HEC under the "hot and wet" condition is relatively higher than that under the "hot and dry" condition. All additional dams tested in this paper are in the Upper Mekong in China (Agent 1), Northern and Central Laos (Agent 4 and 6), and the 3-S basin (Agent 9), these four agents also show the highest impact on baseline HEC under the "hot and wet" condition. These indicate the dam development relatively causing a local effect under the "hot and wet" condition.

5.2. Limitations and potential future work

This study attempts to quantify the impact of dam development and climate change on baseline HEC and NHR to inform better transboundary water resources management. However, we acknowledge
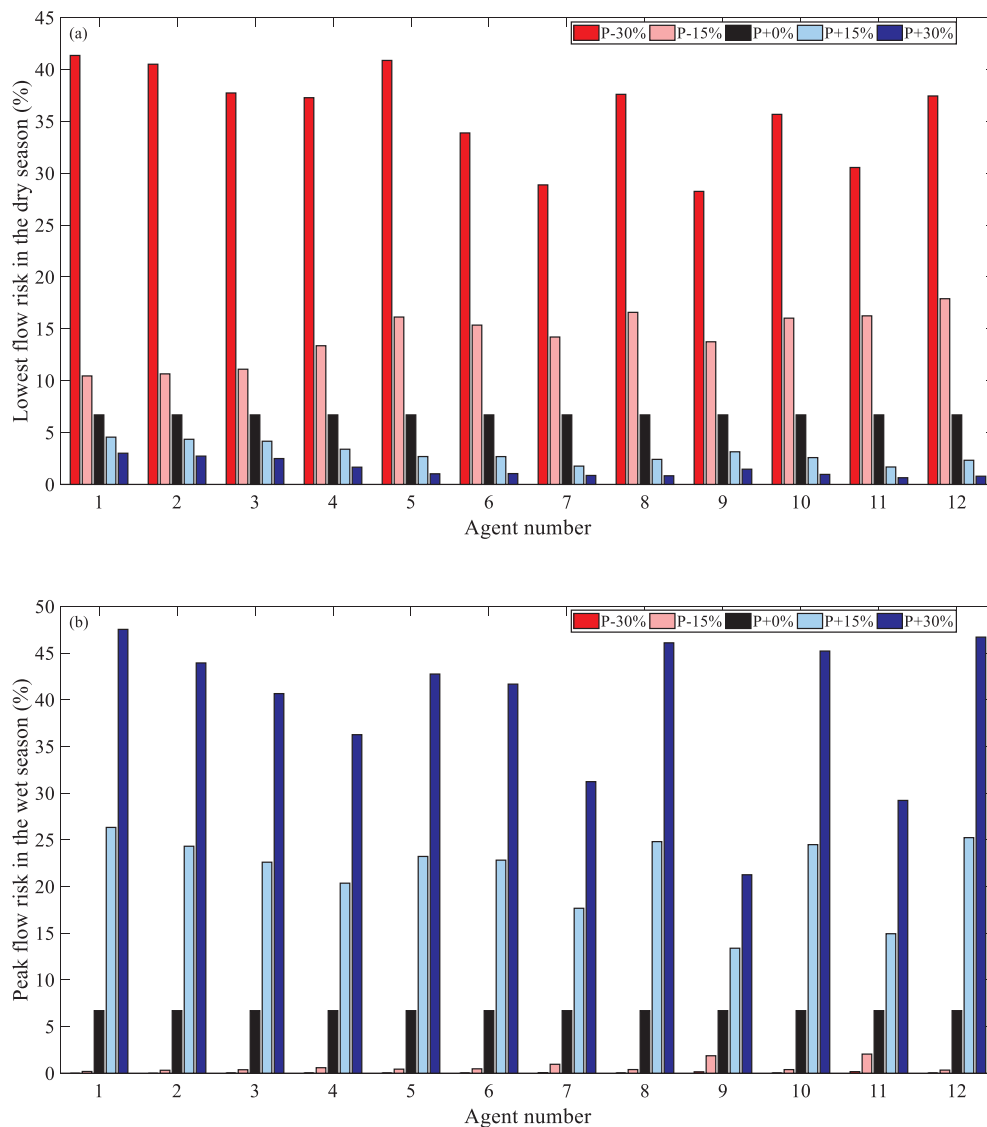
Fig. 7. Precipitation change impact on NHR: (a) for lowest flow event, and (b) for peak flow event. X-axis indicates agent number basically from upstream to downstream. Y-axis is NHR. Blue colors (from light to dark) represent precipitation increase levels. Red colors (from light to dark) represent precipitation decrease levels. Black color represents the precipitation unchanged level.

several limitations that require further evaluations in the future studies.

First, we assume that HEC away from the baseline is less desirable. However, the baseline flow is not necessarily the optimal flow condition to sustain ecosystem health. As desired habitat conditions vary with fish species at a specific time and space (Barbour et al., 2016), more efforts should be devoted to determining the target fish species and its corresponding desired ecological state in each hotspot for better transboundary tradeoff analysis. In addition, the large-scale hydroecological data needed for the relationship analysis may be also be a constraint (Pastor et al., 2014). Second, we only evaluate the impact on streamflow. Dam development and climate change may also result in the relocation of people (Kuenzer et al., 2013), changed irrigation capacity (Kondolf et al., 2014), landscape changes (Zhao et al., 2012), interruption of fish mitigation (Dugan et al., 2010), and biodiversity degradation (Ziv et al., 2012). It is also worth mentioning the sedimentation issue in the MRB. Dams catching sediment have reduced the sediment transport and enlarged the ground subsidence thus leading to the increasing salt-water intrusion in the coastal areas together with the sand extraction and rising sea level caused by global warming (Schmitt et al., 2017). A more comprehensive impact assessment that consider all these aspects caused by dam (when more dams' characteristics

available) and climate change (considering more climatic drivers) is desired but challenging. Third, we simply apply a blanket ratio to the precipitation and temperature record to reflect the possible precipitation and temperature changes. These two climatic drivers' patterns may also change leading to altered flow patterns which should be emphasized in projected climate change impact analysis (Evers and Pathirana, 2018). Furthermore, shorter timescale analyses such as seasonal or even monthly flow abnormal variations in the MRB are important (Li et al., 2018) but ignored in this study. Anomalous conditions (e.g., wet season abnormal low flow) should be further identified throughout the year when the hazard threshold for different time period are determined in each agent. This can provide better support for transboundary policy makings. Besides, other drivers, such as population growth, land use change, urbanization, vegetation deterioration, agricultural expansion that may also affect HEC and NHR (Grumbine et al., 2012) should be considered. Finally, due to data availability limitations, nearly all accessible hydrologic stations located in the mainstream of the MRB will affect the SWAT calibration especially in the large tributaries such as the Agent 7 (Mui River) and Agent 11 (Tonle Sap). The results in these two agents can be misleading such as the very low LAF values shown in Fig. 6. Using these results for policymaking should be avoided.
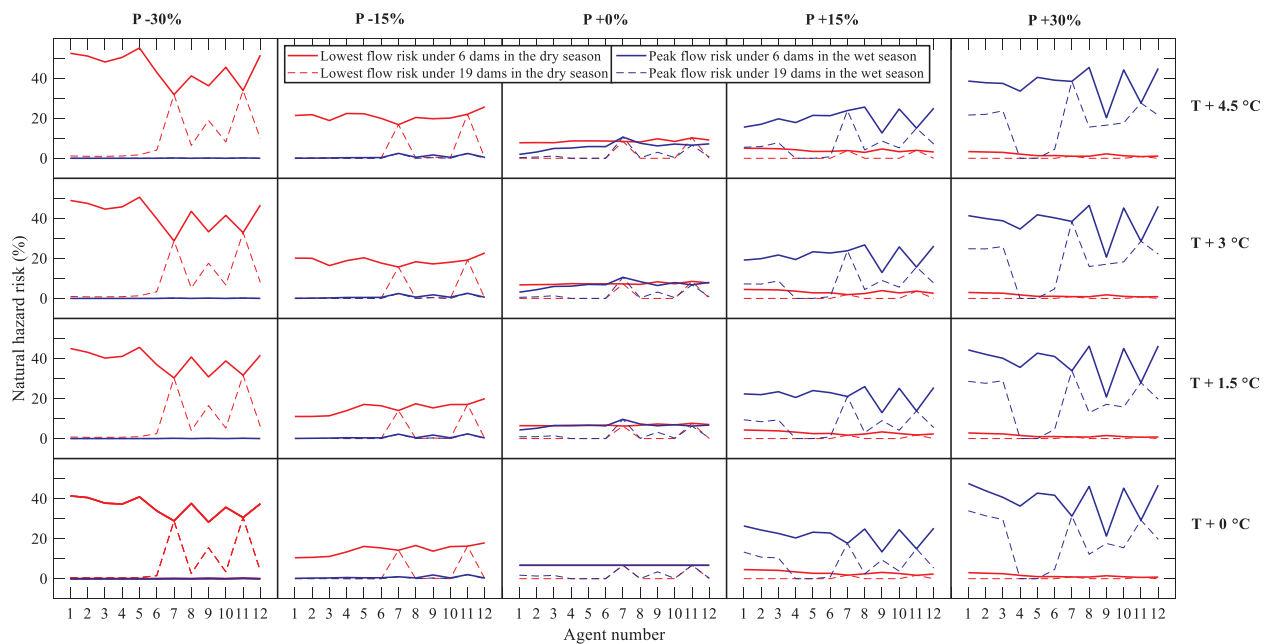
Fig. 8. Joint impact of dam development and climate change on NHR. Diagrams refer to 20 climate change levels. In each diagram, solid red and blue lines represent unacceptable lowest flow and peak flow event risks under no dam development condition, respectively. Dash red and blue lines represent unacceptable lowest flow and peak flow event risks under dam development condition, respectively.

6. Conclusions

Given the rapid industrialization and population growth in the MRB, many dams have been planned or constructed to satisfy growing demands for food, energy and fresh water. These dams, together with climate change, may affect natural flow regimes in ecosystem hotspots and the natural hazard risk in this basin. Some regions may gain benefits while some may experience losses caused by dam development under different climate change conditions, which may escalate geopolitical conflicts in this transboundary river basin. This study assesses the impact of dam development and climate change on baseline local HEC and NHR and then presents the cross-system analysis between HEC and NHR which can be used to inform transboundary policy.

A coupled ABM-SWAT model (Khan et al. 2017a) is applied to

simulate streamflow, dam operation, and irrigation in the basin. Both HEC and NHR are quantified by streamflow results. Forty scenarios, including two with dam development, five with precipitation changes, and four with temperature changes are tested. The modeling results demonstrate that (1) precipitation changes have a greater influence on baseline local HEC and NHR than temperature changes; (2) upstream HEC and NHR variations are more sensitive to precipitation; and (3) negative impacts on baseline local HEC by dam development is more serious under the "hot and wet" condition than the "hot and dry" condition. Under the "hot and wet" extreme climate condition, trade-offs between reduced PFR and increased *CHAD* by dam development in Upper Mekong in China, Northern and Central Laos, and Se San, Sre Pok, and Se Kong basin require special attention. Under the "hot and dry" condition, dam development may reduce the negative impact on
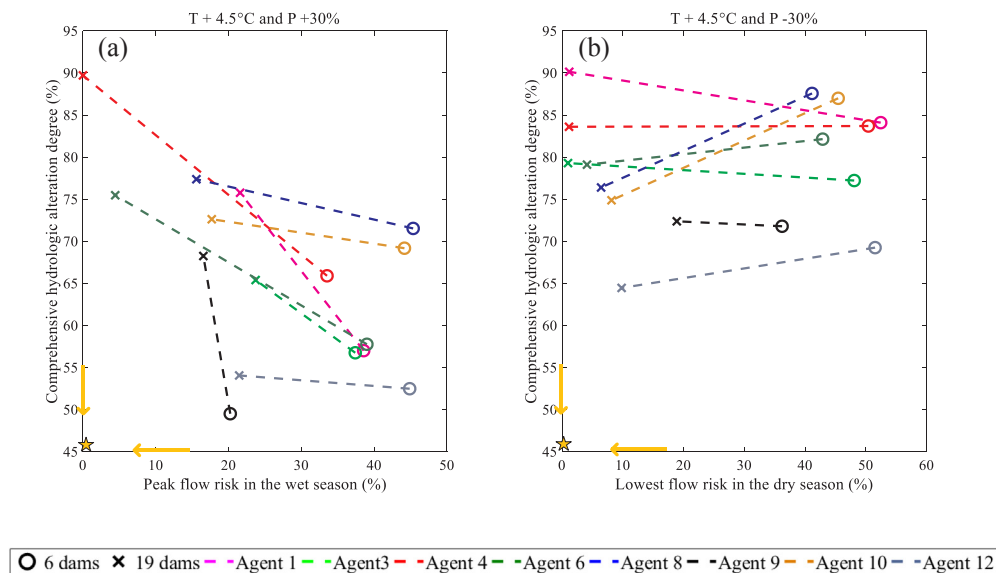

Fig. 9. Tradeoffs between *CHAD* and NHR under two extreme climate change scenarios. The symbols "o" and "x" represent results under baseline and future dam development conditions, respectively.

baseline HEC and LFR in Central and Southern Laos, the Kratie area in Cambodia, and Mekong Delta, if the storage capacity can be used in a flexible manner.

Since the methods employed in this paper are all statistical (the RVA, the IHA, and the NHR calculation), they can potentially be applied to other river basins to support HEC and NHR analyses under changing environments. Future studies should consider a full-scale economic impact analysis, HEC indicators that also include water quality and fish migration, address the sedimentation issue of dam development, and test more exogenous drivers such as humidity, solar radiation, population growth, land use change, agricultural expansion, and irrigation diversion based on the proposed and existing dams.

Declaration of Competing Interest

The authors declare that they have no known competing financial interests or personal relationships that could have appeared to influence the work reported in this paper.

Acknowledgments

Appendix A. Supplementary data

Supplementary data to this article can be found online at https://doi.org/10.1016/j.jhydrol.2019.124177.

References

Angelidis, P., Maris, F., Kotsovinos, N., Hrissanthou, V., 2012. Computation of drought index SPI with alternative distribution functions. Water Resour. Manage. 26 (9), 2453–2473.

Anh, D.T., Hoang, L.P., Bui, M.D., Rutschmann, P., 2018. Modelling seasonal flows alteration in the Vietnamese Mekong Delta under upstream discharge changes, rainfall changes and sea level rise. Int. J. River Basin Manage. 1–15.

Baran, E., Saray, S., Mith, S., 2015. A Fish Perspective on MRC Biodiversity Hotspots in the Mekong Basin. WorldFish Center, Phnom Penh, Cambodia, pp. 24.

Barbour, E.J., Holz, L., Kuczera, G., Pollino, C.A., Jakeman, A.J., Loucks, D.P., 2016. Optimisation as a process for understanding and managing river ecosystems. Environ. Modell. Software 83, 167–178.

Brown, C., Ghile, Y., Laverty, M., Li, K., 2012. Decision scaling: linking bottom-up vulnerability analysis with climate projections in the water sector. Water Resour. Res. 48 (9), W09537. https://doi.org/10.1029/2011WR011212.

Dugan, P.J., Barlow, C., Agostinho, A.A., Baran, E., Cada, G.F., Chen, D., Cowx, I.G., Ferguson, J.W., Jutagate, T., Mallen-Cooper, M., Marmulla, G., Nestler, J., Petrere, M., Welcomme, R.L., Winemiller, K.O., 2010. Fish migration, dams, and loss of ecosystem services in the Mekong basin. Ambio 39 (4), 344–348.

Economist Intelligence Unit, 2017. Water security threats demand new collaborations: Lessons from the Mekong river basin. London: The Economist.

Evers, J., Pathirana, A., 2018. Adaptation to climate change in the Mekong River Basin: introduction to the special issue. Clim. Change 149, 1–11.

Gringorten, I.I., 1963. A plotting rule for extreme probability paper. J. Geophys. Res. 68 (3), 813–814.

Grumbine, R.E., 2018. Using transboundary environmental security to manage the Mekong River: China and South-East Asian Countries. Int. J. Water Resour. Dev. 34 (5), 792–811.

Grumbine, R.E., Dore, J., Xu, J., 2012. Mekong hydropower: drivers of change and governance challenges. Front. Ecol. Environ. 10 (2), 91–98.

Hasson, S., Pascale, S., Lucarini, V., Böhner, J., 2016. Seasonal cycle of precipitation over major river basins in South and Southeast Asia: a review of the CMIP5 climate models data for present climate and future climate projections. Atmos. Res. 180, 42–63.

Hoang, P.L., Lauri, P., Kummu, M., Koponen, J., Van Vliet, M.T., Supit, I., Leemans, H.B.J., Kabat, P., Ludwig, F., 2016. Mekong River flow and hydrological extremes under climate change. Hydrol. Earth Syst. Sci. 20, 3027–3041.

Hoang, L.P., van Vliet, M.T., Kummu, M., Lauri, H., Koponen, J., Supit, I., Leemans, R., Kabat, P., Ludwig, F., 2019. The Mekong's future flows under multiple drivers: how climate change, hydropower developments and irrigation expansions drive hydrological changes. Sci. Total Environ. 649, 601–609.

Intralawan, A., Wood, D., Frankel, R., Costanza, R., Kubiszewski, I., 2018. Tradeoff analysis between electricity generation and ecosystem services in the Lower Mekong Basin. Ecosyst. Serv. 30, 27–35.

Jalilov, S.M., Varis, O., Keskinen, M., 2015. Sharing benefits in transboundary rivers: an experimental case study of Central Asian water-energy-agriculture nexus. Water 7 (9), 4778–4805.

Keskinen, M., Someth, P., Salmivaara, A., Kummu, M., 2015. Water-energy-food nexus in a transboundary river basin: the case of Tonle Sap Lake, Mekong River Basin. Water 7 (10), 5416–5436.

Khan, H.F., Yang, Y.C.E., Xie, H., Ringler, C., 2017a. A coupled modeling framework for sustainable watershed management in transboundary river basins. Hydrol. Earth Syst. Sci. 21 (12), 6275–6288.

Khan, H.F., Yang, Y.C.E., Ringler, C., 2017b. Heterogeneity in Riverine Ecosystem Service Perceptions: Insights for Water-decision Processes in Transboundary Rivers, IFPRI Discussion Paper, Washington, DC.

Kędra, M., Wiejaczka, Ł., 2018. Climatic and dam-induced impacts on river water temperature: assessment and management implications. Sci. Total Environ. 626, 1474–1483.

Kingston, D.G., Thompson, J.R., Kite, G., 2011. Uncertainty in climate change projections of discharge for the Mekong River Basin. Hydrol. Earth Syst. Sci. 15 (5), 1459–1471.

Kondolf, G.M., Rubin, Z.K., Minear, J.T., 2014. Dams on the Mekong: cumulative sediment starvation. Water Resour. Res. 50 (6), 5158–5169.

Kontgis, C., Schneider, A., Ozdogan, M., Kucharik, C., Duc, N.H., Schatz, J., 2019. Climate change impacts on rice productivity in the Mekong River Delta. Appl. Geogr. 102, 71–83.

Kuenzer, C., Campbell, I., Roch, M., Leinenkugel, P., Tuan, V.Q., Dech, S., 2013. Understanding the impact of hydropower developments in the context of upstream–downstream relations in the Mekong river basin. Sustain. Sci. 8 (4), 565–584.

Kummu, M., Sarkkula, J., 2008. Impact of the Mekong River flow alteration on the Tonle Sap flood pulse. AMBIO: J. Human Environ. 37 (3), 185–193.

Lacombe, G., Douangsavanh, S., Baker, J., Hoanh, C.T., Bartlett, R., Jeuland, M., Phongpachith, C., 2014. Are hydropower and irrigation development complements or substitutes? The example of the Nam Ngum River in the Mekong Basin. Water Int. 39 (5), 649–670.

Lauri, H., Moel, H.D., Ward, P.J., Räsänen, T.A., Keskinen, M., Kummu, M.S., 2012. Future changes in Mekong River hydrology: impact of climate change and reservoir operation on discharge. Hydrol. Earth Syst. Sci. 16, 4603–4619.

Le, T.V.H., Nguyen, H.N., Wolanski, E., Tran, T.C., Haruyama, S., 2007. The combined impact on the flooding in Vietnam's Mekong River delta of local man-made structures, sea level rise, and dams upstream in the river catchment. Estuar. Coast. Shelf Sci. 71 (1–2), 110–116.

Li, D., Long, D., Zhao, J., Lu, H., Hong, Y., 2017. Observed changes in flow regimes in the Mekong River basin. J. Hydrol. 551, 217–232.

Li, D., Wan, W., Zhao, J., 2018. Optimizing environmental flow operations based on explicit quantification of IHA parameters. J. Hydrol. 563, 510–522.

Matthews, N., Motta, S., 2015. Chinese state-owned enterprise investment in Mekong hydropower: political and economic drivers and their implications across the water, energy, food nexus. Water 7 (11), 6269–6284.

Mekong River Commission (MRC), 2010. State of the Basin Report 2010. Mekong River Commission, Vientiane, Laos PDR.

Nalbantis, I., Tsakiris, G., 2009. Assessment of hydrological drought revisited. Water Resour. Manage. 23 (5), 881–897.

Ngo, L.A., Masih, I., Jiang, Y., Douven, W., 2018. Impact of reservoir operation and climate change on the hydrological regime of the Sesan and Srepok Rivers in the Lower Mekong Basin. Clim. Change 149 (1), 107–119.

Pastor, A.V., Ludwig, F., Biemans, H., Hoff, H., Kabat, P., 2014. Accounting for environmental flow requirements in global water assessments. Hydrol. Earth Syst. Sci. 18 (12), 5041–5059.

Piman, T., Cochrane, T.A., Arias, M.E., Green, A., Dat, N.D., 2012. Assessment of flow changes from hydropower development and operations in Sekong, Sesan, and Srepok rivers of the Mekong basin. J. Water Resour. Plann. Manage. 139 (6), 723–732.

Pittock, J., Dumaresq, D., Bassi, A.M., 2016. Modeling the hydropower-food nexus in large river basins: a Mekong case study. Water 8 (10), 425.

Räsänen, T.A., Koponen, J., Lauri, H., Kummu, M., 2012. Downstream hydrological impacts of hydropower development in the Upper Mekong Basin. Water Resour. Manage. 26 (12), 3495–3513.

Räsänen, T.A., Varis, O., Scherer, L., Kummu, M., 2018. Greenhouse gas emissions of hydropower in the Mekong River Basin. Environ. Res. Lett. 13 (3), 034030.

Richter, B.D., Baumgartner, J.V., Braun, D.P., Powell, J., 1998. A spatial assessment of hydrologic alteration within a river network. Regulated Rivers: Res. Manage. 14 (4), 329–340.

Richter, B.D., Baumgartner, J.V., Powell, J., Braun, D.P., 1996. A method for assessing hydrologic alteration within ecosystems. Conserv. Biol. 10 (4), 1163–1174.

Richter, B.D., Baumgartner, J.V., Wigington, R., Braun, D., 1997. How much water does a river need? Freshw. Biol. 37 (1), 231–249.

Ringler, C., Karelina, Z., Pandya-Lorch, R., 2011. Emerging country strategies for improving food security: linkages and trade-offs for water and energy security. Bonn 2011 Conference: The Water, Energy, and Food Security Nexus, Bonn, Germany.

Ruan, Y., Liu, Z., Wang, R., Yao, Z., 2019. Assessing the performance of CMIP5 GCMs for projection of future temperature change over the lower mekong basin. Atmosphere 10 (2), 93.

Saha, S., Moorthi, S., Pan, H., 2010. NCEP Climate Forecast System Reanalysis (CFSR) Selected Hourly Time-Series Products, January 1979 to December 2010. Research Data Archive at the National Center for Atmospheric Research, Computational and Information Systems Laboratory. https://doi.org/10.5065/D6513W89. Accessed 06/03/2019.

Schmitt, R.J.P., Rubin, Z., Kondolf, G.M., 2017. Losing ground-scenarios of land loss as consequence of shifting sediment budgets in the Mekong Delta. Geomorphology 294, 58–69.

Shiau, J.T., Wu, F.C., 2004. Assessment of hydrologic alterations caused by Chi-Chi diversion weir in Chou-Shui Creek, Taiwan: opportunities for restoring natural flow conditions. River Res. Appl. 20 (4), 401–412.

Shrestha, B., Babel, M.S., Maskey, S., Griensven, A.V., Uhlenbrook, S., Green, A., Akkharath, I., 2013. Impact of climate change on sediment yield in the Mekong River basin: a case study of the Nam Ou basin, Lao PDR. Hydrol. Earth Syst. Sci. 17 (1), 1–20.

Shrestha, S., Bach, T.V., Pandey, V.P., 2016. Climate change impacts on groundwater resources in Mekong Delta under representative concentration pathways (RCPs) scenarios. Environ. Sci. Policy 61, 1–13.

Shrestha, B., Maskey, S., Babel, M.S., van Griensven, A., Uhlenbrook, S., 2018. Sediment related impacts of climate change and reservoir development in the Lower Mekong River Basin: a case study of the Nam Ou Basin, Lao PDR. Clim. Change 149 (1), 13–27.

Tian, Y., Zhang, K., Xu, P., Gao, X., Wang, J., 2018. Evaluation of potential evapotranspiration based on CMADS reanalysis dataset over China. Water 10 (9), 1126.

Thompson, J.R., Green, A.J., Kingston, D.G., Gosling, S.N., 2013. Assessment of uncertainty in river flow projections for the Mekong River using multiple GCMs and hydrological models. J. Hydrol. 486, 1–30.

Trisurat, Y., Aekakkararungroj, A., Ma, H.O., Johnston, J.M., 2018. Basin-wide impacts of climate change on ecosystem services in the Lower Mekong Basin. Ecol. Res. 33 (1), 73–86.

Van Loon, A.F., 2015. Hydrological drought explained. Wiley Interdiscip. Rev. Water 2 (4), 359–392.

Vu, D.T., Yamada, T., Ishidaira, H., 2018. Assessing the impact of sea level rise due to climate change on seawater intrusion in Mekong Delta, Vietnam. Water Sci. Technol. 77 (6), 1632–1639.

Wen, X., Liu, Z., Lei, X., Lin, R., Fang, G., Tan, Q., Wang, C., Tian, Yu., Quan, J., 2018. Future changes in Yuan River ecohydrology: individual and cumulative impacts of climates change and cascade hydropower development on runoff and aquatic habitat quality. Sci. Total Environ. 633, 1403–1417.

Yang, Y.C.E., Ringler, C., Brown, C., Mondal, M.A.H., 2016. Modeling the agricultural water–energy–food nexus in the Indus River Basin, Pakistan. J. Water Resour. Plan. Manage. 142 (12), 04016062.

Yatagai, A., Kamiguchi, K., Arakawa, O., Hamada, A., Yasutomi, N., Kitoh, A., 2012. APHRODITE: constructing a long-term daily gridded precipitation dataset for Asia based on a dense network of rain gauges. Bull. Am. Meteorol. Soc. 93 (9), 1401–1415.

Yen, N.T.H., Sunada, K., Oishi, S., Ikejima, K., 2008. Tonle sap ecosystem fish species biological groups and hydroecological index. Int. J. Ecol. Econ. Statist. 66–81.

Yu, Y., Zhao, J., Li, D., Wang, Z., 2019. Effects of hydrologic conditions and reservoir operation on transboundary cooperation in the Lancang-Mekong River Basin. J. Water Resour. Plann. Manage. 145 (6), 04019020.

Zhao, Q., Liu, S., Deng, L., Dong, S., Yang, Z., Yang, J., 2012. Landscape change and hydrologic alteration associated with dam construction. Int. J. Appl. Earth Obs. Geoinf. 16, 17–26.

Ziv, G., Baran, E., Nam, S., Rodríguez-Iturbe, I., Levin, S.A., 2012. Trading-off fish biodiversity, food security, and hydropower in the Mekong River Basin. Proc. Natl. Acad. Sci. 109 (15), 5609–5614.